OPTICAL STUDIES OF THE MORPHOLOGICAL CHANGES IN DEFORMING POLYOLEFINS

R. S. STEIN, MARION B. RHODES, P. R. WILSON and SUE N. STIDHAM
Department of Chemistry, University of Massachusetts, Amherst, Mass., U.S.A.

INTRODUCTION

This article is a presentation of progress of studies of the crystalline superstructure in high polymers by the light-scattering and microscopic techniques. In previous review articles[1, 2], it was pointed out that the scattering is a consequence of regions of correlated orientation of crystal–amorphous aggregates with dimensions comparable with the wavelength of light. In this paper more recent progress is reviewed. Much of this is centred about the use of the photographic procedure for recording the angular distribution of low-angle scattering, particularly at small angles. The use of the optical diffractometer technique for interpreting scattering pictures is discussed. Comparison of information obtained by light-scattering and optical and electron microscopy is made.

REVIEW OF EARLIER WORK

Procedures and preliminary studies of the scattering from thin polymer films have been described by Stein and Keane[3, 4]. (A computer technique for easily obtaining absolute scattered intensities from experimental data has been recently developed[5].) It was concluded that scattering at angles greater than 10° results principally from regions within the polymer containing crystallites having correlated orientation over regions of several thousand Å in size. This conclusion is in agreement with the results of studies of:

(a) polarization of the scattered light;
(b) changes in scattering accompanying the swelling with solvents of differing refractive index; and
(c) changes in scattering accompanying the melting and regrowth of crystals.

The existence of such regions is consistent with current mechanisms of crystallization[6] involving growth through autonucleation of crystals in regions close to those already containing crystals. It is proposed that crystalline orientation tends to be preserved in this autonucleation process.

A description of such crystalline superstructure in terms of a correlation function for orientation has been proposed[2, 7, 8], which specifies the probability of two crystals with correlated orientation occurring in volume elements separated by distance r. By employing simplifying assumptions (with some loss of generality), it is experimentally possible to separate contributions to scattering resulting from such fluctuations in orientation from those resulting from fluctuations in density or degree of crystallinity. This requires the

measurement of scattering intensities using polarized light. It has been found, in this way, that most of the scattering from polyethylene films originates from orientation fluctuations.

THE PHOTOGRAPHIC TECHNIQUE

A simple photographic method for recording scattering patterns at low angles has been described[9, 10], utilizing the experimental arrangement shown in *Figure 1.* The scattering pattern is observed as a function of the radial

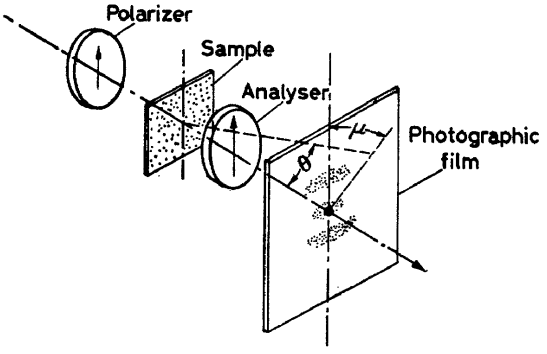

Figure 1. The experimental arrangement for photographic light-scattering from films (Stein and Rhodes[10] by courtesy *J. Appl. Phys.*)

angle, θ, and the azimuthal angle, μ, for cases where the polarizer and analyser are parallel and vertical (V_V scattering), and where they are perpendicular (H_V scattering). One observes complex angular dependency of the scattering pattern which is oriented with respect to the polarization direction (*Figure 2*). The pattern may be understood in terms of scattering from an anisotropic system having circular symmetry. A theory for such scattering from isolated spheres having differing radial and tangential polarizability has been presented[10], giving rise to the equations for the scattered intensity, I, for V_V and H_V polarization:

$$I_{V_V} = Av_0^2\left(\frac{3}{U^3}\right)^2\Big[(\alpha_t - \alpha_s)(2\sin U - U\cos U - \mathrm{Si}U) + (\alpha_r - \alpha_s')(\mathrm{Si}U - \sin U) + (\alpha_t - \alpha_r)\cos^2\frac{\theta}{2} \times \cos^2\mu(4\sin U - U\cos U - 3\mathrm{Si}U)\Big]^2 \qquad (1)$$

$$I_{H_V} = Av_0^2\left(\frac{3}{U^3}\right)^2\Big[(\alpha_t - \alpha_r)\cos^2\frac{\theta}{2}\sin\mu\cos\mu(4\sin U - U\cos U - 3\mathrm{Si}U)\Big]^2 \qquad (2)$$

where A is a proportionality constant; $(\alpha_t - \alpha_s')$ is the difference between the tangential polarizability and that of the surroundings of the sphere,

$(\alpha_r - \alpha_s')$ is this difference for the radial polarizability, and $(\alpha_t - \alpha_r)$ is the difference between the tangential and radial polarizabilities; v_0 is the volume of the sphere of radius R; and $U = \left(\frac{4\pi R}{\lambda}\right)\sin(\theta/2)$, where λ is the wavelength of light in the medium. Similar equations have been derived[11] for anisotropic discs lying in the plane of the film, and are:

$$I_{V_V} = BA_0^2\left(\frac{2}{\omega^2}\right)^2\Big\{(\alpha_t - \alpha_s)[\omega J_1(\omega) + J_0(\omega) - 1] + (\alpha_r - \alpha_s')[1 - J_0(\omega)] + (\alpha_t - \alpha_r)[2 - 2J_0(\omega) - \omega J_1(\omega)]\cos^2\mu\Big\}^2 \quad (3)$$

$$I_{H_V} = BA_0^2\left(\frac{2}{\omega^2}\right)^2\Big\{(\alpha_t - \alpha_r)\sin\mu\cos\mu[2 - 2J_0(\omega) - \omega J_1(\omega)]\Big\}^2 \quad (4)$$

where B is a proportionality constant; A_0 = area of the thin disc of radius R; $\omega = 2\pi(R/\lambda)\sin\theta$; and $J_0(\omega)$ and $J_1(\omega)$ are Bessel functions of the first kind of order zero and one respectively.

For isotropic surroundings, α_s and α_s' are the same. In most actual cases, however, the structure is close-packed so that crystalline aggregates are surrounded by other similar aggregates which are anisotropic, and the meaning of α_s and α_s' is not clear.

The theoretically predicted scattering patterns for H_V scattering from spheres and discs are very similar. In *Figure 3*, a calculated scattering contour (obtained using the IBM 1620 computer of the University of Massachusetts Research Computing Center), is plotted for discs showing the variation in intensity with ω and μ. The lines represent levels of constant logarithmic intensity (with the value of logarithmic intensity indicated). The pattern is very similar to ones obtained for spheres (see *Figure 7* of the paper by Stein and Rhodes[10]), and has the four-leaf clover symmetry found experimentally.

A greater variety of shape is found in the V_V patterns. These depend upon the relative values of the polarizabilities as well as upon the shape of the scattering aggregate. For example, in *Figures 4* and *5*, the scattering for spheres and discs is compared for the relative polarizability differences $(\alpha_t - \alpha_r) = 3$, $(\alpha_t - \alpha_s) = 1$, and $(\alpha_r - \alpha_s') = -2$. The patterns are of very different appearance. In *Figure 6*, the scattering for spheres for which $(\alpha_t - \alpha_r) = 3$, $(\alpha_t - \alpha_s) = 2$, and $(\alpha_r - \alpha_s') = -1$ is plotted. The pattern again differs for, in this case, the intensity decreases from a maximum at $\mu = 90°$, as U increases from 0, rather than increasing as in *Figure 4*.

Variations of this sort are found in practice. For example, a comparison of the V_V and H_V scattering patterns from nylon films cooled rapidly and slowly from the melt is made in *Figure 7*. The birefringence of nylon spherulites is known to depend upon the temperature of growth[27], and the difference in the scattering patterns is associated with polarizability differences accompanying the birefringence variation.

A more systematic study of the effect of polarizabilities on scattering patterns has been made, and variations in scattering patterns have been reported[11].

It has been pointed out[10] that the distance from the centre of the scattering pattern to one of the 45° lobes of the H_V " clover-leaves " may be taken as a measure of the size of the scattering aggregate. A calculation of the variation of I_{H_V} with U using equation (2) for spheres or with ω using equation (4) for discs indicates maximum intensity at $U = \omega = 4{\cdot}0$. At small angles, this gives, for both shapes:

$$\frac{R}{\lambda} = \frac{2}{\pi \sin\theta_{max}} \tag{5}$$

where θ_{max} is the angular position of the intensity maximum. A measurement of R in this way gives values which correlate well with average spherulite sizes measured with a polarizing microscope[10]. Three H_V scattering patterns for differing polyethylene spherulite sizes are shown in *Figure 8*. The agreement of the R values characteristic of the scattering aggregate with measured spherulite sizes makes the association of the aggregate with the spherulite reasonable. It should be noted that R values may be readily measured in this manner for samples possessing spherulites which are too small to be resolved with an optical microscope. From the nature of their scattering patterns, it is probable that such samples possess " spheruliticlike " aggregates of crystals, even though these cannot be observed.

The physical explanation for the orientation of the V_V scattering patterns with respect to the polarization direction may be understood from a study of *Figure 9*. This represents an idealized sphere with zero radial polarizability; that is, the electrons are only free to move in a tangential direction. The arrows represent the magnitude of the induced dipoles when this sphere is placed in vertically polarized light. It is seen that the polarization is greatest in the equatorial regions of the sphere. Thus, the sphere acts as an anisotropically-shaped scattering body giving a scattering pattern which is most extended in a direction perpendicular to the direction of greatest extension of the dipoles[12].

EFFECT OF DISTRIBUTION OF SPHERULITE SIZES

It is of interest to determine the effect of a distribution of spherulite sizes upon the H_V and V_V scattering patterns. If the number of spherulites with radii between R and $(R + dR)$ is $\mathcal{N}(R)dR$), the total H_V scattering from spheres is, from equation (2):

$$I_{H_V} = 16\pi^2 A \int \mathcal{N}(R) \left\{ \frac{R^3}{U^3} \left[(\alpha_t - \alpha_r)\cos^2\frac{\theta}{2}\sin\mu\cos\mu \right] \right.$$
$$\left. [4\sin U - U\cos U - 3\mathrm{Si}U] \right\}^2 dR \tag{6}$$

If $C = 16\pi^2 A(\alpha_t - \alpha_r)^2\cos^4(\theta/2)\sin^2\mu\cos^2\mu$, and $U = hR$

where $h = 4\pi\sin(\theta/2)\lambda$, then this becomes:

$$I_{H_V} = C \int \mathcal{N}(R) \frac{1}{h^6}[4\sin(hR) - (hR)\cos(hR) - 3\mathrm{Si}(hR)]^2 dR \tag{7}$$

This permits one to calculate I_{H_V} as a function of h (or θ) for a known

distribution $\mathcal{N}(R)$. This integral was evaluated numerically for the two assumed values of $\mathcal{N}(R)$:

(a) Gaussian, where $\mathcal{N}(R) = \exp\left[-\left(\frac{R - R_0}{a}\right)^2\right]$ (where R_0 is the most probable radius in Gaussian distribution or maximum radius in box distribution, and a is the width of Gaussian distribution, the correlation distance for fluctuations); and

(b) box sketched in *Figure 10*,

using the IBM 1620 computer.

The resulting scattering curves are compared with those for monodisperse spherulites of 10 μ radius. They are plotted as a function of ($U_0 = hR_0$), where $R_0 = 10$ μ is the most probable radius in the Gaussian distribution and the maximum radius in the box distribution (*Figure 11*). It is seen that, while there are small shifts in the position of the maximum, the shape of the scattering curve is not appreciably affected by the distribution of sizes. The average size calculated using equation (5) would be 10 μ for the monodisperse distribution, 12·1 μ for the Gaussian and 8·5 μ for the box distribution. The average size obtained is heavily weighted in favour of the larger sizes in the distribution because of the dependency of scattering power upon R^6.

The result for V_V scattering depends upon the assumptions concerning α_s and α_s'. If, as in the case of isotropic surroundings, $\alpha_s = \alpha_s' = (\alpha_r + 2\alpha_t)/2$, (scattering pattern of *Figure 4*) one obtains from equation (1) at $\mu = 90°$:

$$I_{V_V}(\mu = 90°) = 16\pi A(\alpha_t - \alpha_s)^2 \int \mathcal{N}(R)\frac{R^6}{U^6}[4\sin U - U\cos U - 3\mathrm{Si}U]^2 dR \quad (8)$$

The predicted variation with U is the same as that for I_{H_V} as given by equation (6), and the effect of distributions of spherulite size upon the scattering curve will be the same.

In the case where $(\alpha_r - \alpha_s') = -(\alpha_t - \alpha_s)/2$, (which seems to give V_V scattering patterns of the type shown in *Figure 6* having similar appearance to the experimental pattern for the sample studied), equation (1) leads to:

$$I_{V_V}(\mu = 90°) = 4\pi^2 A(\alpha_t - \alpha_s)^2 \int \mathcal{N}(R)\frac{R^6}{U^6}[5\sin U - 2U\cos U - 3\mathrm{Si}U]^2 dR \quad (9)$$

A plot of this function for the Gaussian distribution:

$$\mathcal{N}(R) = \exp[-(R - R_0)^2/a^2]$$

is given in *Figure 12* for monodisperse spheres ($a = 0$) and for $a = 1$ and 5 μ, and $R_0 = 10$ μ. It is seen that the sharp minima in the curve for monodisperse particles become more diffuse with increasing breadth of distribution of particle sizes. Thus, in this case, in calculating a particle size from the angular dependency of scattering, the influence of broadening on the scattering curve must be considered.

In the theory used, the surrounding medium was considered as homogeneous, and contributions to scattering due to interparticle interferences were ignored. The justification of this may be made in terms of the

conclusion that scattering in the region of small θ ultimately results in a scattering minimum occurring at $\theta = 0°$, and a maximum at an angle characteristic of interparticle interference. " The positions and magnitudes of the secondary maxima are only slightly modified in passing from a very dilute to a dense system. This is not true for the principal maximum; the principal maximum occurs at zero angle for dilute solutions, and as the concentration increases, it is displaced towards larger angles, occurring at values of U between 0 and 2·5 for systems of average concentration "[13]. Such maxima are not observed experimentally. Evidence for the effect of interparticle interference will be presented in the following section on the optical diffraction technique. More detailed discussions of the effect of particle size on scattering will be reported elsewhere[14].

OPTICAL DIFFRACTOMETER STUDIES

A quantitative treatment of the effect of interparticle interaction on scattering is difficult. However, a qualitative appraisal of the effects of this interaction may be made using the optical diffractometer technique[15,16]. The method involves making a two-dimensional drawing of the structure which is proposed to be responsible for the light-scattering. A diffraction mask is prepared photographically from this drawing. The enlarged diffraction pattern obtained using this mask should then be similar to the light-scattering pattern arising from the actual structure.

An example of the application of this technique is illustrated in *Figures 13* and *14*. An idealized model of a spherulite as viewed through a horizontal analyser in vertically-polarized light is shown in *Figure 13*. The white areas represent the region of high concentration of dipoles as seen through the analyser arising, as previously discussed, because of the anisotropy of polarizability of the tangentially-polarizable spherulite. The large scattering occurs at 45° to the polarizer and analyser because the maximum component of polarization (which is greatest in a direction at 90° to the polarizer) is transmitted through the analyser at 45°. For simplicity, the spherulite is divided into two zones, the white which contains dipoles and the black which does not. This is an idealization of the actual spherulite which contains a gradient of polarization. *Figure 14* represents a close-packed array of such spherulites with some variation in their size.

The diffraction patterns corresponding to those two models are shown in *Figures 15* and *16*. (The patterns were obtained by Professor S. Krimm of the Department of Physics, University of Michigan, Ann Arbor, Michigan.) The pattern, as is predicted, exhibits the cross pattern found experimentally. The single spherulite pattern is similar to that for the array, with the exception that there is more diffuseness in the array pattern, probably resulting in part from the variation in size of spherulites in the array and in part from the incompleteness of spherulites with irregular edges where they abut other spherulites. The intensity of the array pattern is greater than that of the single spherulite because of the greater number of scatterers.

INTERNAL RING STRUCTURE

The appearance of concentric rings in spherulites has been observed under the polarizing microscope, and has been explained in terms of the

helicoidal variation in the orientation of crystals within the spherulites, the angular orientation varying periodically with radius[17–19]. The scattering patterns from such "ringed spherulites" exhibit a maximum[20, 21]. The existence of such a maximum is theoretically predicted[10], and the dependency of the intensity of the scattering maximum upon the azimuthal scattering angle with V_V polarization confirms the postulate of periodically varying orientation.

The effect of ring structure on the scattering from an array of spherulites has been examined using the optical diffractometer technique[16]. One finds that the scattering maximum obtained from an array is similar to that obtained from a single spherulite, but that its intensity is greater, and the angular width is broader.

CHANGES ON HEATING AND COOLING

When molten polyethylene is cooled, the scattered intensity exhibits a maximum at a temperature slightly below the melting point[2, 22, 23]. This maximum has been studied by the photographic technique[10, 23] using polarized light. It has been proposed that the maximum results from the refractive index difference between spherulitic and amorphous material, the effect of which is a maximum when the polymer is about half-spherulitic. With further crystallization, the spherulites become volume-filling and scattering decreases. With still further crystallization, there is an increase in scattering. The photographic patterns reveal that the intensity of V_V scattering in the region of the first scattering maximum is independent of azimuthal angle, but that the pattern accompanying this second increase is highly oriented along the polarization direction as in *Figure 2*. The interpretation is that this second increase is a consequence of the development of anisotropy resulting from intraspherulitic crystallization. The growth of spherically symmetric oriented crystals within the spherulite causes $(\alpha_t - \alpha_r)$ to increase and gives rise to an increasing contribution from the third term of equation (1) which is dependent upon the azimuthal angle, μ. Consequently, the scattering which is observed at room temperature arises almost entirely from this cause.

INTERNAL STRUCTURE

The light-scattering consequences of helicoidal crystal orientation within spherulites have been already discussed. These studies indicate that spherulites do not have perfectly uniform internal composition, but are internally heterogeneous as a result of their polycrystalline structure. A consequence of this is that there is a much greater intensity of scattering at high angles than would be predicted for uniform spheres. For example, for a medium-density polyethylene sample, the average size of spherulites calculated using equation (5) from the position of the H_V scattering maximum at $\mu = 45°$ was 2·7 μ. (This is in agreement with estimates from microscopic observations.) For spheres of this size, the calculated logarithm of the ratio of the intensity at $\theta = 3°$ to that at 10° (using equation (9)) is between about 1·3 and 2·0, depending upon the assumed width of distribution of spherulite sizes. The experimentally measured logarithmic intensity ratio at these angles is 3·9. Thus, the actual intensity at 10° is

over a hundred times as great as might be expected for internally homogeneous spherulites.

The observation that a sample of polyethylene which is of the order of 50 per cent crystalline may have its volume completely filled with spherulites indicates that spherulites may exist having degrees of crystallinity 50 per cent or less. It is of interest to inquire into the scale of mixing of crystalline and amorphous material within the spherulite.

One means for estimating the size of the amorphous regions is from the effect of swelling on the intensity of scattered light. This depends upon the size of the scattering regions and upon the square of the refractive index difference between them and their surroundings[24]. The size may be obtained from the dependency of the intensity of scattering upon angle. Such a measurement on low-density polyethylene at angles in the range of 10–30° has indicated a size of about 0·26 μ and a mean square refractive index difference, $\overline{\eta^2}$, of $2{\cdot}9 \times 10^{-4}$ for a sample of about 50 per cent crystallinity[4].

Since

$$\overline{\eta^2} = X_1 X_2 (n_1 - n_2)^2 \tag{10}$$

and X_1 and X_2 and n_1 and n_2 are the fractions and refractive indices, respectively, of the scattering system which is assumed to consist of two phases, this corresponds to $(n_1 - n_2)$ of the order of 0·01 refractive index units.

One may swell this polymer with 23 per cent tetralin having a refractive index of 1·545. Since the crystalline X-ray diffraction pattern is unchanged upon swelling, all of the tetralin must enter the amorphous phase. Its concentration in the amorphous phase must be of the order of 46 per cent. Assuming a linear change of refractive index with concentration, at an initial amorphous refractive index of 1·49, the refractive index of the amorphous regions should change by 0·03 to a value of about 1·52. The change in refractive index produced by the swelling liquid is three times the refractive index difference which is responsible for the scattering. There is no significant change in the size of the scattering region upon swelling. The observed change in scattering at 10° is less than 10 per cent. Consequently, the amorphous–crystalline boundary cannot be a significant contributor to the scattering.

If all the observed scattering were due to the refractive index difference between crystalline and amorphous material having a refractive index difference of 0·05, then the value of $\overline{\eta^2}$ calculated with equation (10) would be 0·006 refractive index units. Then, one may estimate the size of the scattering regions by using the integrated form of the Debye-Bueche equation[24] for an exponential correlation function:

$$\boldsymbol{R} = \frac{4\pi\overline{\eta^2}}{\lambda_0^4} \frac{a^3}{(1 + k^2 s^2 a^2)^2} (1 + \cos^2\theta) \tag{11}$$

where $\boldsymbol{R}$ is the Rayleigh ratio, a the correlation distance, λ_0 the wavelength in vacuum, $k = 2\pi/\lambda$ and $s = 2 \sin(\theta/2)$. Using the measured value of $\boldsymbol{R}$ of about 20 cm^{-1} for such a sample[4], one obtains an a value of about 900 Å. From the swelling studies, however, it does not seem that more than 10 per cent of the scattering can be due to the refractive index difference between

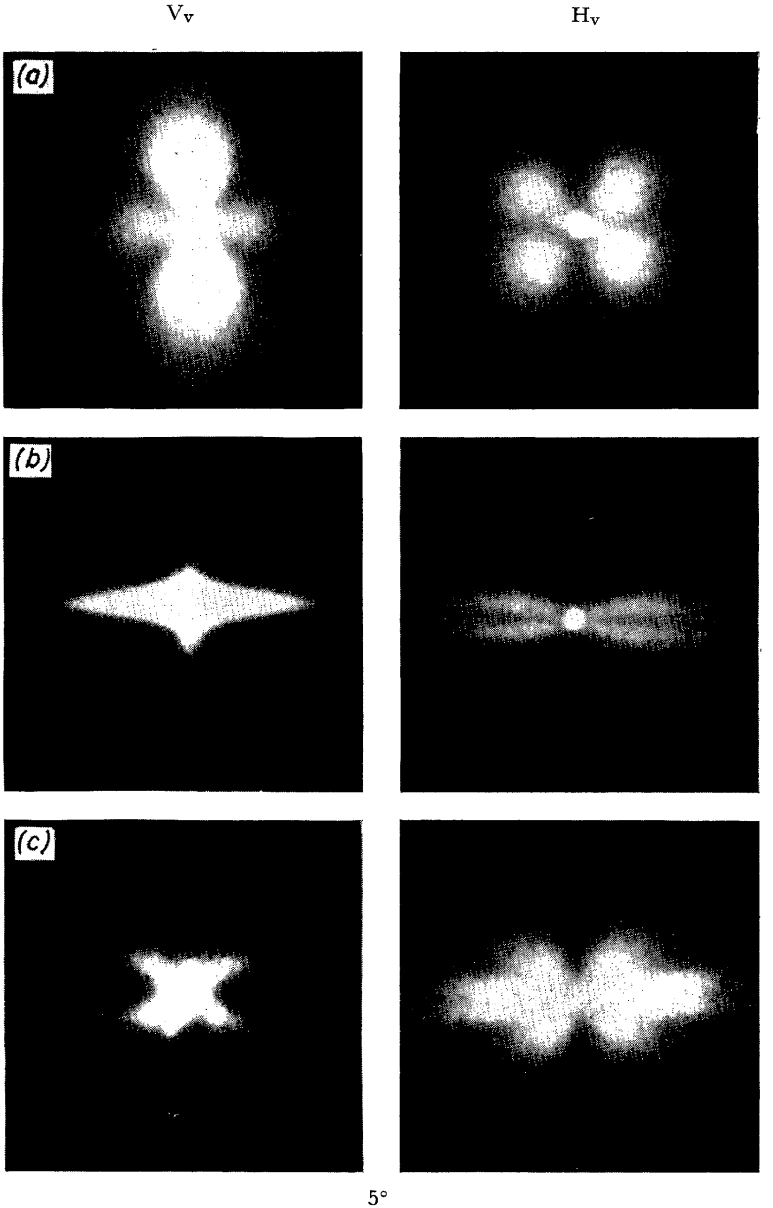

Figure 2. The photographic light-scattering patterns for a medium-density polyethylene sample with V_V and H_V polarization. The line under the pictures represents 5° of scattering angle: (*a*) unstretched sample; (*b*) sample stretched 400 per cent vertically; (*c*) sample annealed for 1 h at 102° without constraint on length and then cooled to room temperature

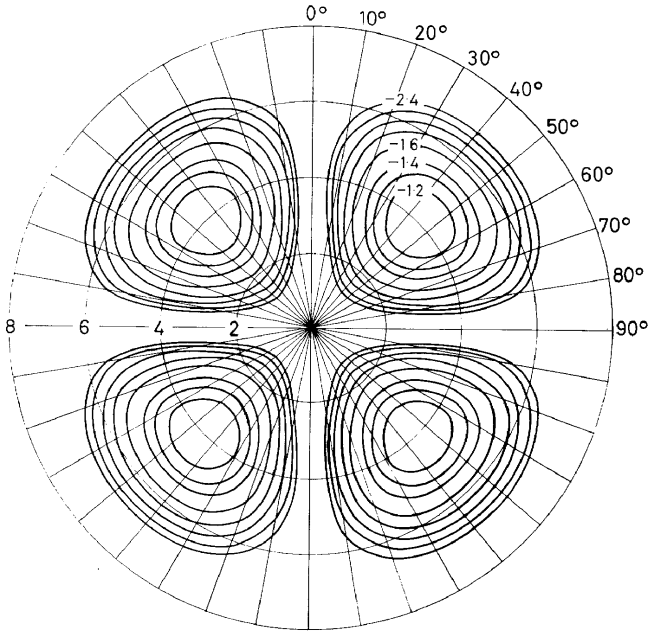

Figur 3. Logarithmic intensity contours for H_v scattering from thin discs where $(\alpha_t - \alpha_r) = 3$

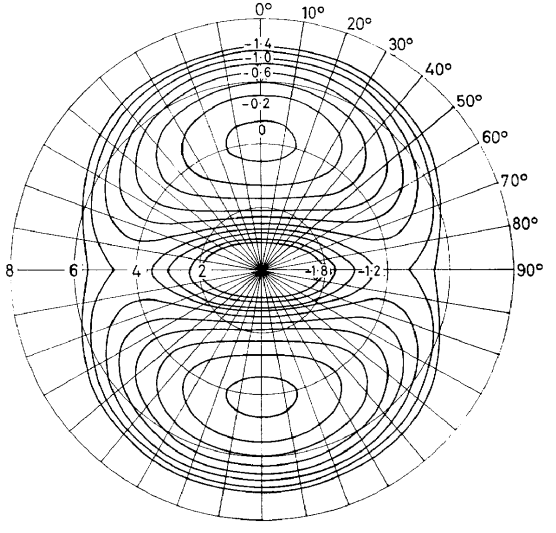

Figure 4. Logarithmic intensity contours for V_v scattering from spheres where $(\alpha_t - \alpha_r) = 3$, $(\alpha_t - \alpha_s) = 1$ and $(\alpha_r - \alpha_s') = -2$. (This corresponds to $\alpha_s = \alpha_s' = (\alpha_r + 2\alpha_t)/2$)

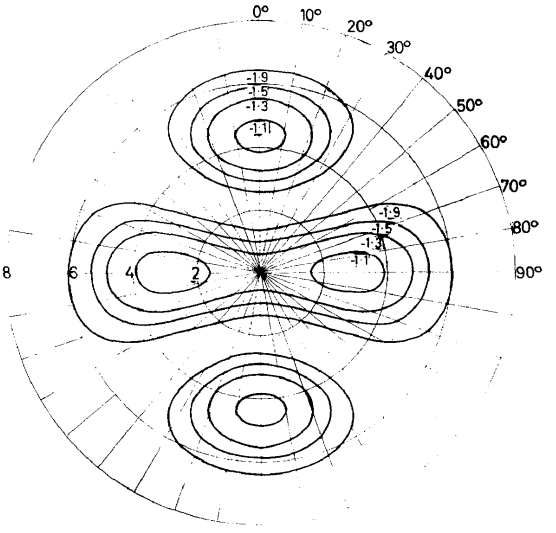

Figure 5. Logarithmic intensity contours for V_v scattering from thin discs where $(\alpha_t - \alpha_r) = 3$, $(\alpha_t - \alpha_s) = 1$ and $(\alpha_r - \alpha_s') = -2$ (this corresponds to $\alpha_s = \alpha_s' = (\alpha_r + 2\alpha_t)/2$.)

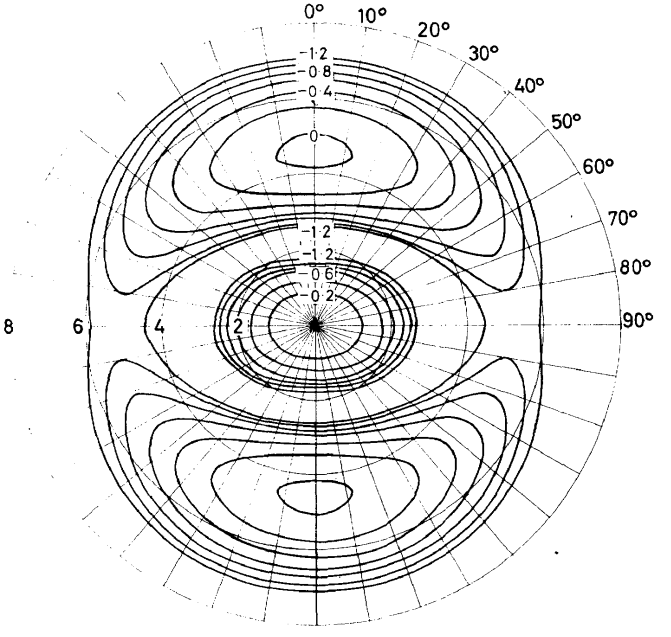

Figure 6. Logarithmic intensity contours for V_V scattering from spheres where $(\alpha_t - \alpha_r) = 3$, $(\alpha_t - \alpha_s) = 2$ and $(\alpha_r - \alpha_s') = -1$

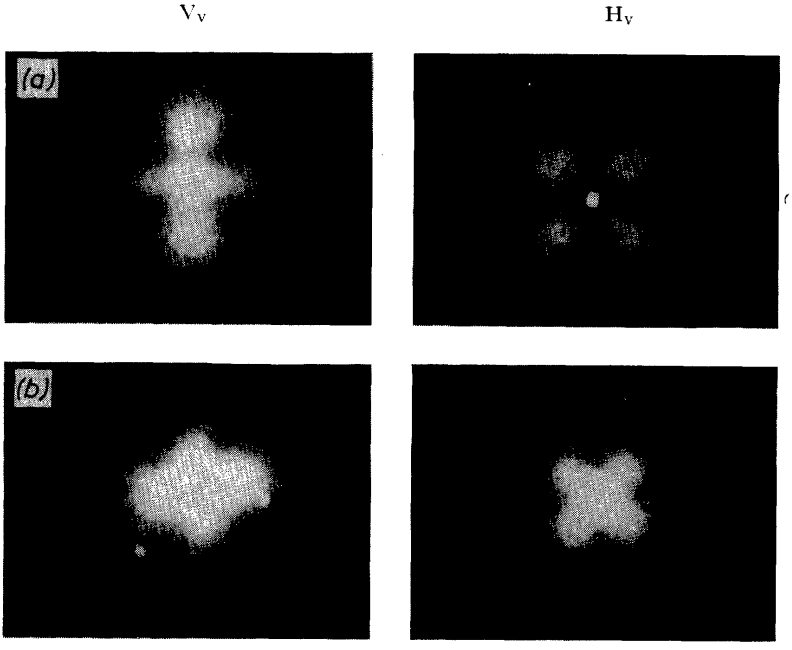

Figure 7. V_V and H_V scattering patterns for nylon films (*a*) cooled rapidly and (*b*) cooled slowly from the melt

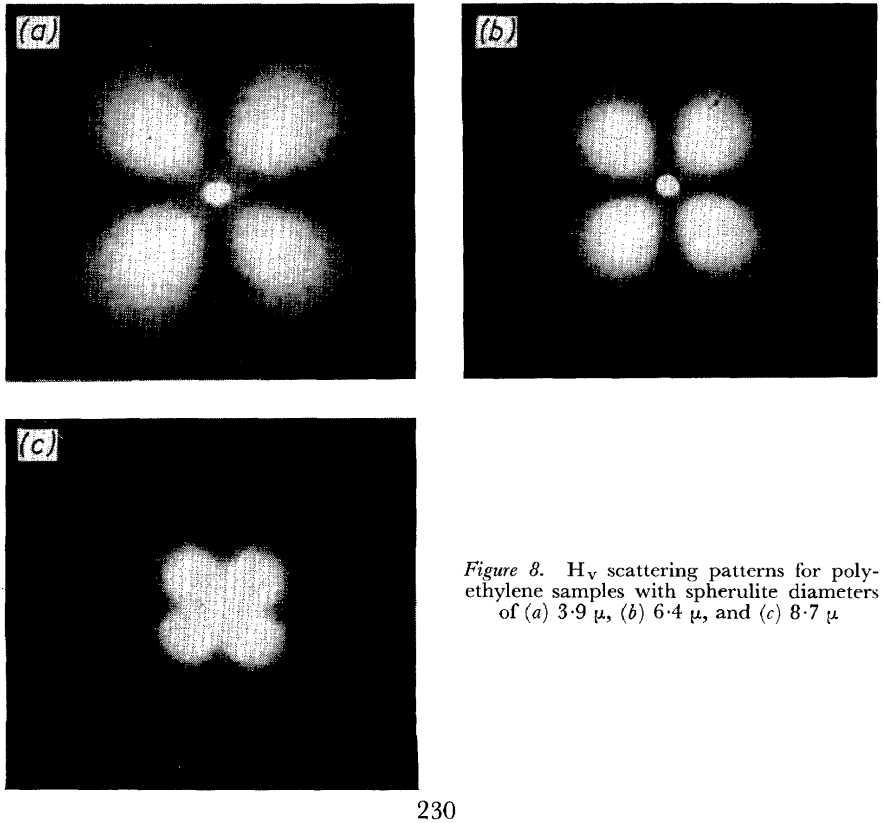

Figure 8. H_V scattering patterns for polyethylene samples with spherulite diameters of (*a*) 3·9 μ, (*b*) 6·4 μ, and (*c*) 8·7 μ

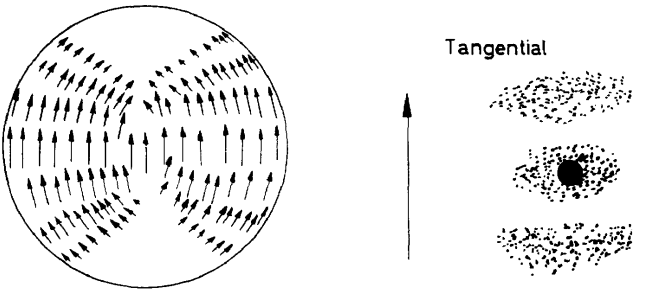

Figure 9. The distribution of induced dipoles in a tangentially-polarizable spherulite in vertically-polarized light

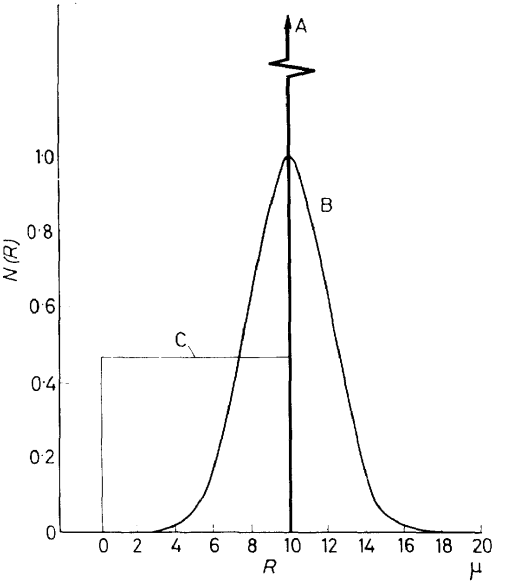

Figure 10. The assumed distribution functions for spherulite sizes corresponding to: A, monodisperse distribution, $R = 10$ μ; B, Gaussian distribution, $R_0 = 10$ μ, $a = 3$ μ; and C, box distribution, $R_{min} = 0{\cdot}1$ μ, $R_{max} = 10$ μ

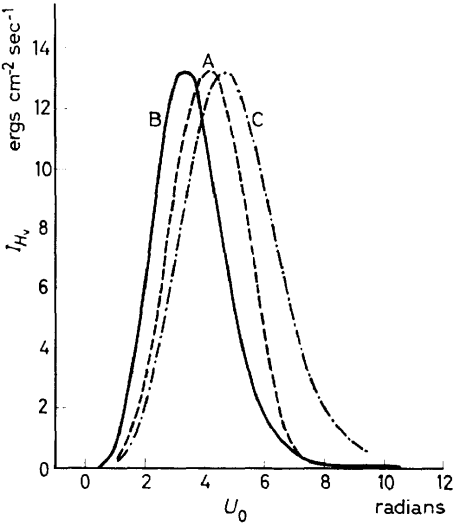

Figure 11. The calculated dependency of the H_V intensity on U_0 for: A, monodisperse distribution; B, Gaussian distribution; and C, box distribution

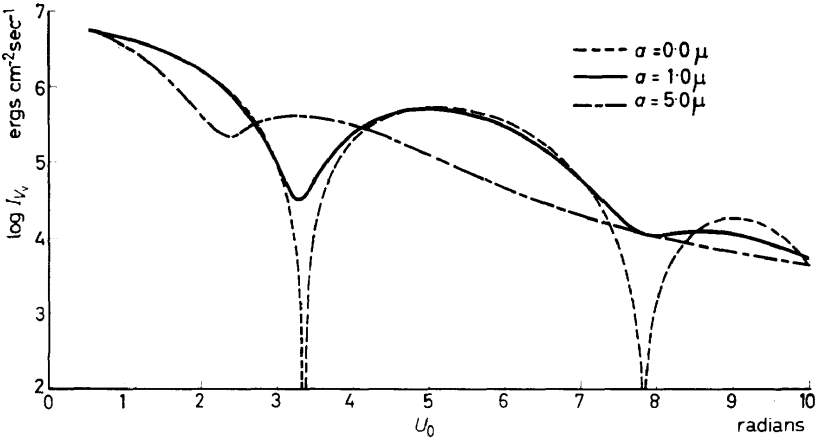

Figure 12. The calculated dependency of the V_V intensity on U_0

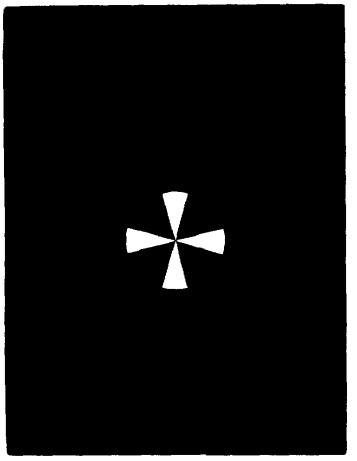

Figure 13. The optical diffraction mask for an isolated tangentially-polarizable spherulite between crossed polaroids (H_V scattering). The polarizer and analyser lie at 45° to the vertical and at 90° to each other

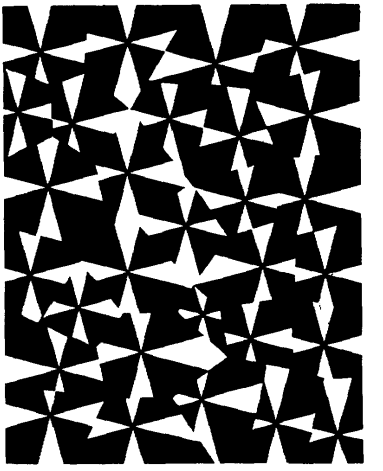

Figure 14. The optical diffraction mask for an array of spherulites like that in *Figure 13* (H_V polarization)

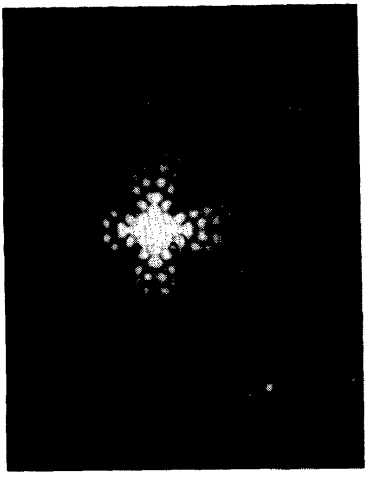

Figure 15. The optical diffraction pattern from the diffraction mask of *Figure 13* for a single spherulite with H_V polarization (Wilson, Krimm and Stein[16]. By courtesy *J. Phys. Chem.*)

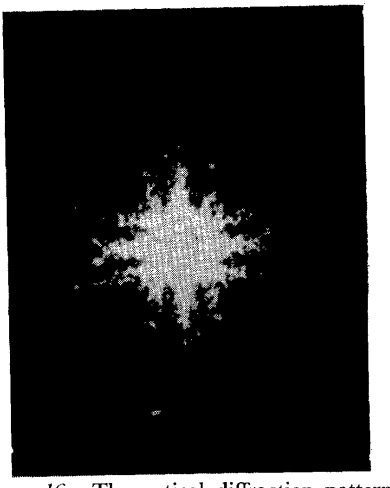

Figure 16. The optical diffraction pattern from the diffraction mask of *Figure 14* for an array of spherulites with H_V polarization (Wilson, Krimm and Stein[16]. By courtesy *J. Phys. Chem.*)

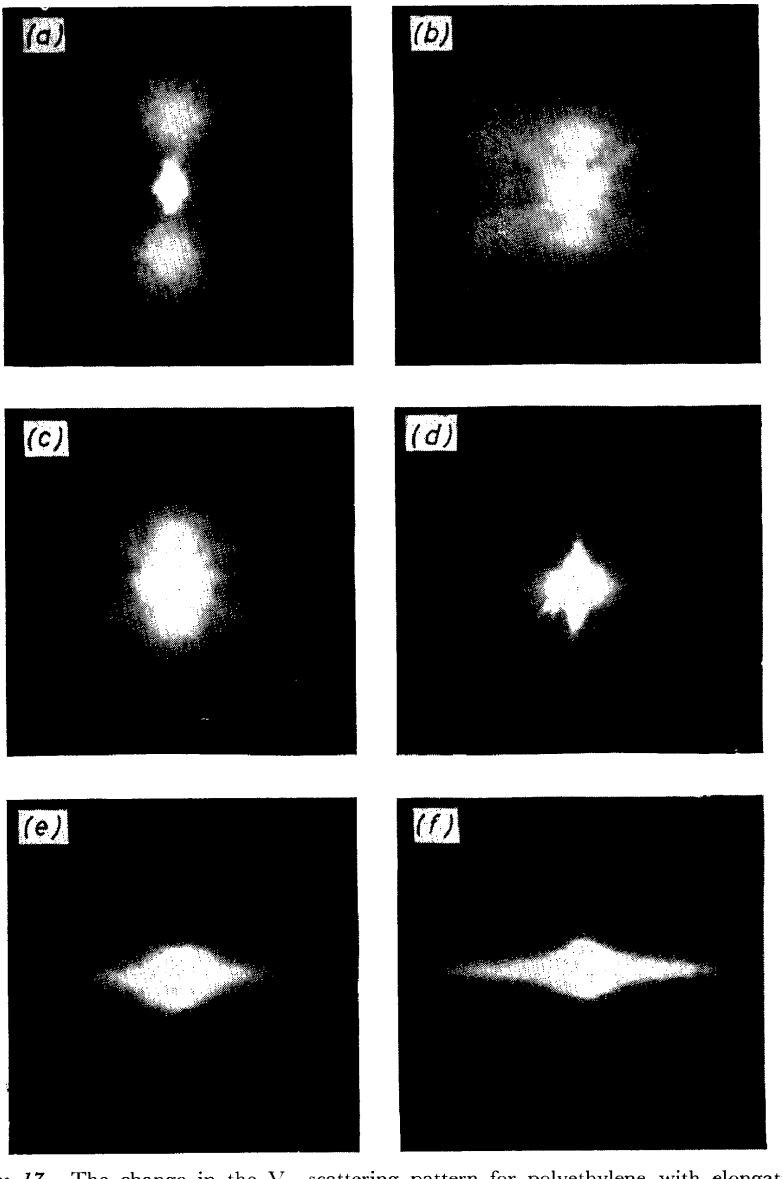

Figure 17. The change in the V_V scattering pattern for polyethylene with elongation: (*a*), no elongation; (*b*), 25 per cent elongation; (*c*), 50 per cent elongation; (*d*), 100 per cent elongation; (*e*), 125 per cent elongation; (*f*), 300 per cent elongation. The stretching direction is vertical

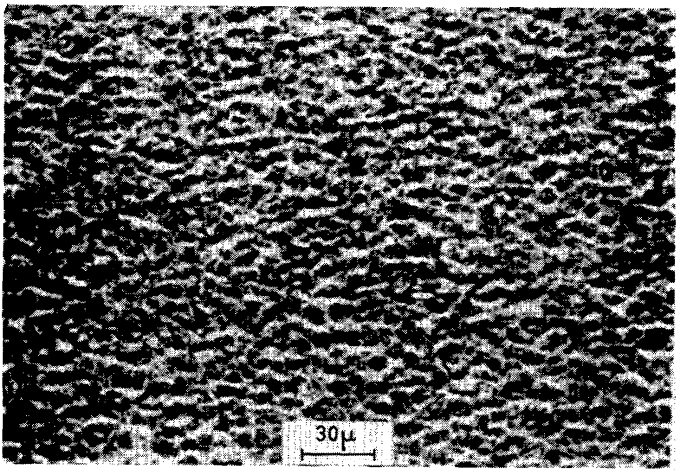

Figure 18. Phase-contrast microscope picture of an undrawn polyethylene film

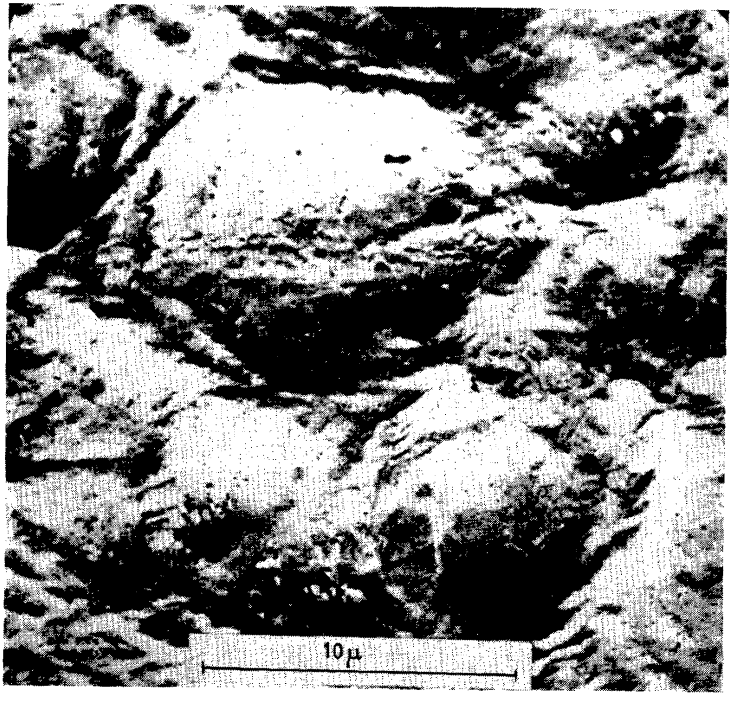

Figure 19. Electron-micrograph (shadowed surface replica) of an undrawn portion of a polyethylene film showing spherulite structure

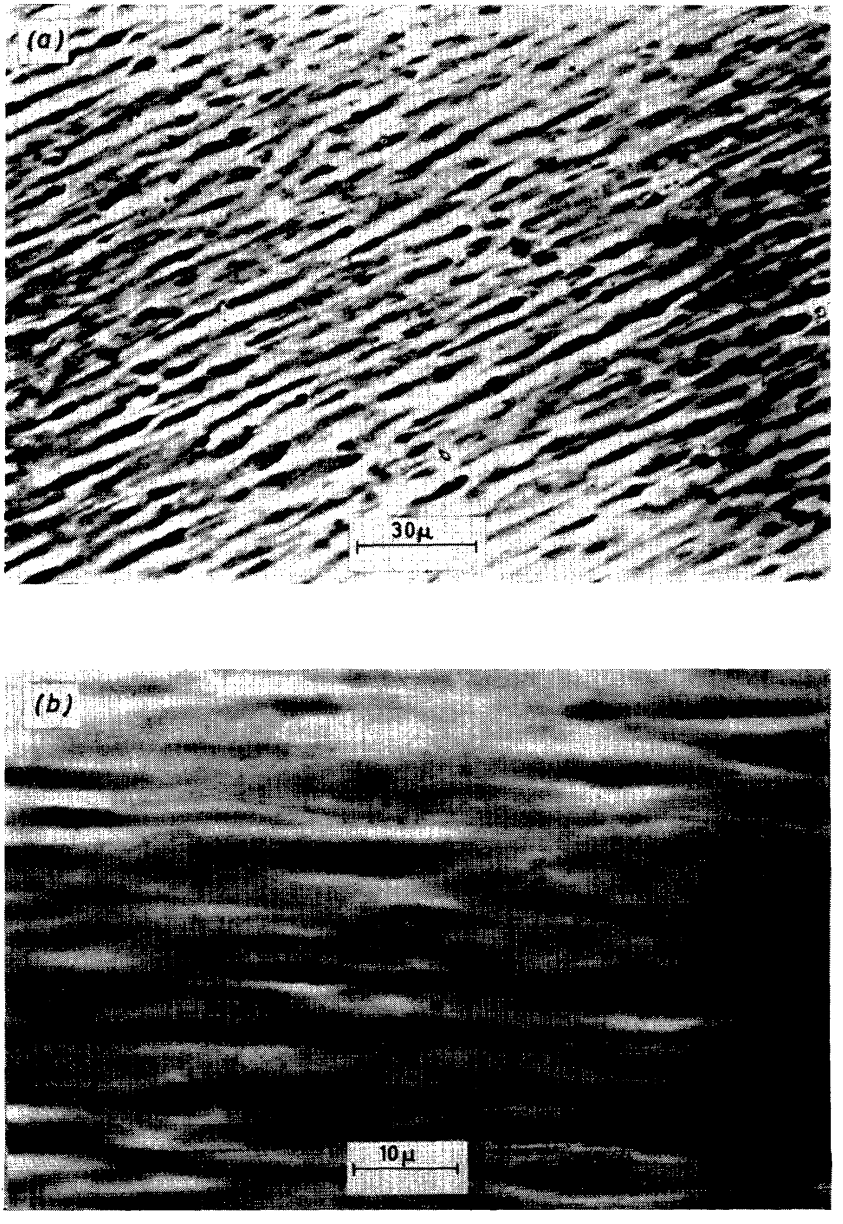

Figure 20. Phase-contrast micrographs of polyethylene films stretched 250–350 per cent at two magnifications

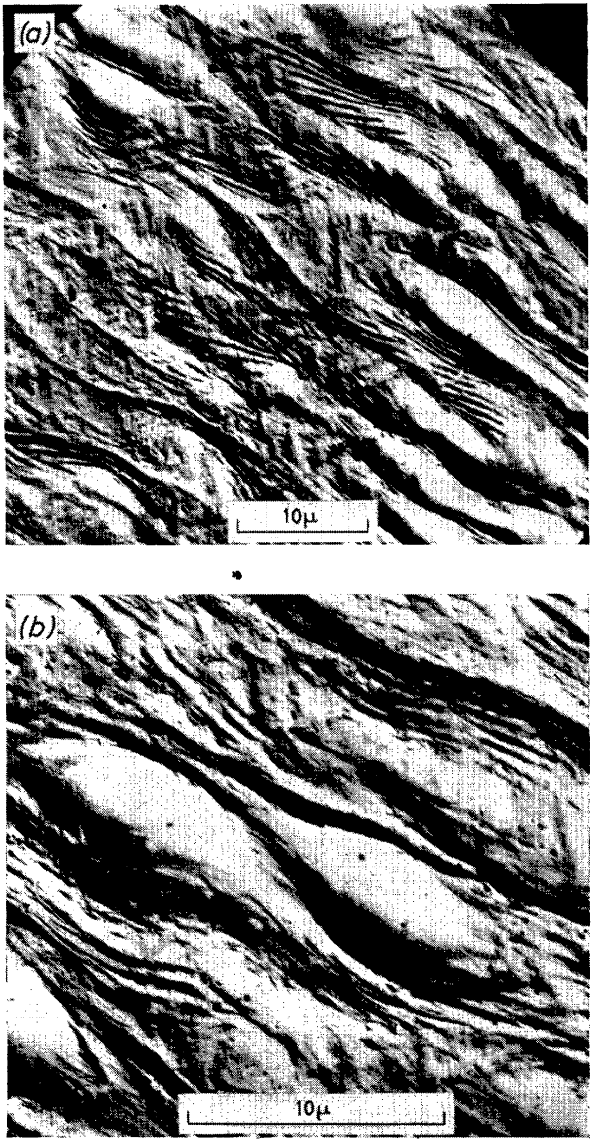

Figure 21. Two magnifications of electron-micrograph of a 100 per cent stretched polyethylene film

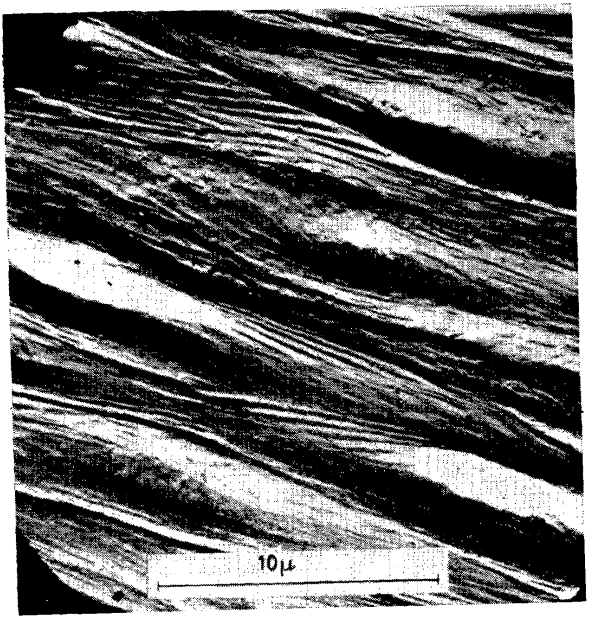

Figure 22. Electron-micrograph of a 400 per cent stretched polyethylene film

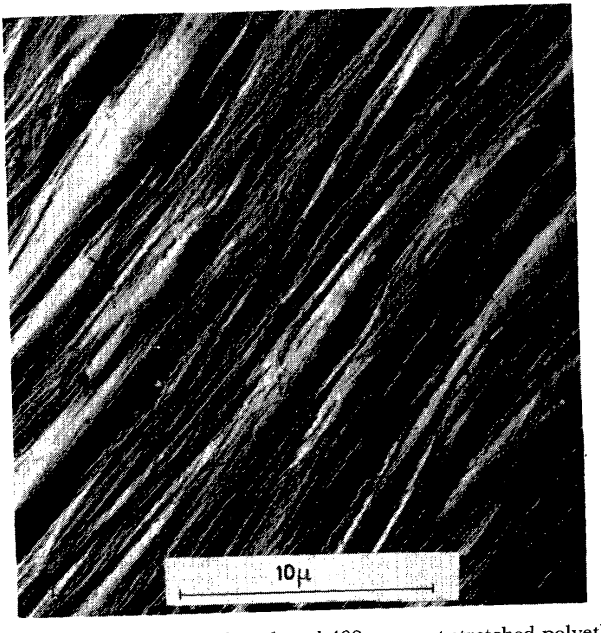

Figure 23. Electron-micrograph of a relaxed 400 per cent stretched polyethylene film

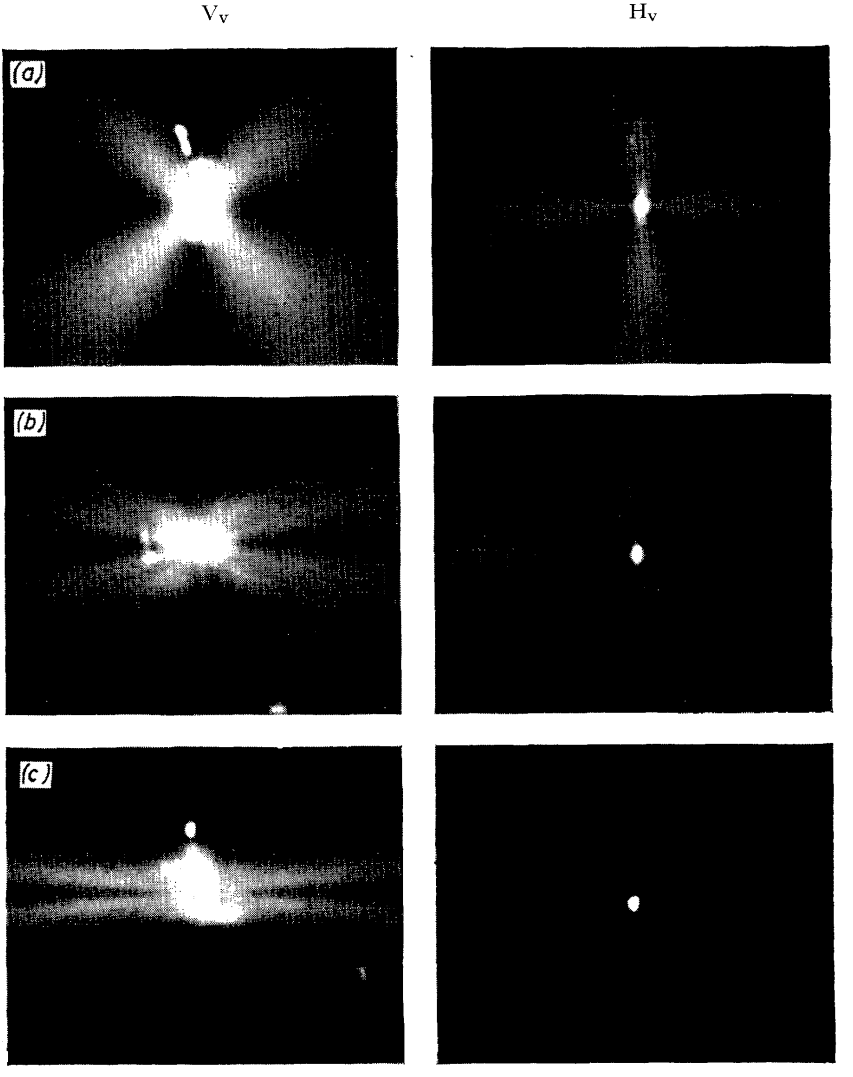

Figure 24. V_V and H_V light-scattering patterns for Teflon films at a series of elongations: (*a*), no elongation; (*b*), 60 per cent elongation; (*c*) 200 per cent elongation

crystalline and amorphous regions, so that the contribution to the Rayleigh ratio from this cause cannot be more than 2 cm^{-1}. This would limit a to around 300 Å. It is probable that more precise measurements would lead to a lower value.

The result of 300 Å is comparable with crystal size measurements obtained by low-angle X-ray diffraction and from the width of wide-angle diffraction peaks. In a 50 per cent crystalline polymer, the size of crystals and amorphous regions is about the same.

The correlation distances obtained for low-density polyethylene are of the order of 3000 Å. It has been concluded that most of the scattering arising from internal spherulitic structure originates from fluctuations in orientation of the constituent crystals[1, 2]. It would appear that correlation in orientation occurs within groups of crystals having linear dimensions of the order of 5–10 times the crystal size.

A model for the internal structure of a spherulite has been tested by the optical diffraction technique[16]. Two states of orientation were assumed, and it was postulated that crystals in a particular state of orientation were more likely to occur in the neighbourhood of similarly oriented crystals. This resulted in a diffraction mask containing clusters of crystals of common orientation. The diffraction pattern from this mask had an angular dependency similar to that observed for scattered intensities at higher angles.

EFFECT OF STRETCHING

It has been shown that both the low-angle[10] and wide-angle[25] scattering patterns change appreciably upon stretching the polymer. The wide-angle pattern changes were associated with the orientation of the clusters of crystals along the common stretching direction. The low-angle patterns exhibited complex changes which depended upon the state of polarization of the light[26]. For example, *Figure 17* shows the changes in the V_V scattering patterns for a polyethylene sample stretched parallel to the polarization direction. One first observes a distortion of the V_V pattern in the range of 0–25 per cent elongations. With further stretching, a cross-like pattern becomes superposed upon the two-lobe V_V spherulite pattern. With still further stretching, the spherulite-type pattern decreases in intensity while the cross opens up and changes into a horizontal streak characteristic of scattering from a fibrous structure having its greatest polarizability in the stretching direction. Thus, the scattering patterns reflect the transition from a spherulitic to a fibrous structure.

An attempt was made to observe changes in phase-contrast optical microscope and electron microscope pictures paralleling the light-scattering changes. *Figure 18* shows a phase-contrast picture of an unstretched sample similar to that studied by light-scattering. The graininess characteristic of spherulites 10 μ or less in diameter is apparent. A shadowed electron-micrograph of a surface replica of an unstretched portion of a similar sample is shown in *Figure 19**, in which the spherulitic structure is more obvious. Two magnifications of phase-contrast pictures of stretched portions of this

*The electron-micrographs were made through the co-operation of the Monsanto Chemical Co. (Plastics Division), Springfield, Mass., with the collaboration of Mr R. J. Clark and assistance of Mr W. Golba.

material are seen in *Figure 20*. The drawing-out of the spherulites is apparent and the development of a " herring-bone " striated texture in the drawn portion is seen in the higher magnification picture.

The striations are more apparent in the electron-micrographs. *Figures 21(a)* and *21(b)* show two magnifications of shadowed surface replicas of a 100 per cent stretched sample, while *Figure 22* is for a 400 per cent stretched sample. The development of the striated regions and the decrease in the angle between the striations and the stretching direction with stretching is seen. The preceding micrographs are all for samples held under strain. In *Figure 23*, the result of releasing the strain on a 400 per cent elongated sample is shown. The material appears to become even more fibrous with the striations aligned almost parallel to the stretching direction. Distorted remnants of the original spherulites are seen, but these are only about one-fifth of the size of the spherulites in the unstretched sample.

It is postulated that the cross-type scattering pattern results from the striated regions developing from the drawn spherulites. The co-existence of the two types of scattering patterns at intermediate elongations is associated with the co-existence of distorted undrawn and striated drawn material. The decrease in the intensity of the spherulite-type scattering pattern with increasing elongation is related to the decrease in size of the undrawn regions, while the transition from a cross to a horizontal streak is associated with the alignment of the striations along the stretching direction.

Complex changes in scattering patterns occurring upon annealing have been reported[26]. For example, in *Figure 2*, V_V and H_V patterns for unstretched, stretched and annealed polyethylene samples are shown where the stretching direction is vertical. The additional structure developed in the H_V pattern for the annealed sample is associated with recrystallization of the drawn structure upon annealing. The microscopic study of these changes is now in progress.

Complex variations of scattering patterns with elongation have also been observed. For example, in *Figure 24*, changes in the V_V and H_V patterns accompanying the elongation of Teflon film are present. The orientation of the H_V and V_V patterns in the unstretched material differs greatly from that for polyethylene (*cf. Figure 2*). With Teflon, the H_V scattering pattern is most intense along the polarization direction while the V_V pattern has its maximum at $\mu = 45°$. It would appear that this would be characteristic of a non-spherulitic structure in which the direction of greatest polarizability was oriented at an angle to the direction of greatest extension of correlated dipoles.

Summary

The photographic technique for studying light-scattering patterns from polymer films is reviewed. Calculations are presented for the scattering from spheroidal and disc-like aggregates of crystals of differing polarizabilities, and comparison is made with experiment. The use of the optical diffractometer technique for interpreting scattering pictures is discussed. Comparison of information obtained by light-scattering and optical and electron microscopy is made.

This project was supported in part by a contract with the Office of Naval Research, and grants from the Plax Corporation, Petroleum Research Foundation, Monsanto Chemical Company, and Fabric Research Laboratories.

References

[1] R. S. Stein. " Morphology of Crystalline Aggregates in Polyethylene ", in *Growth and Perfection of Crystals* (Eds. R. H. Doremus, B. W. Roberts and D. Turnbull), p. 549, Wiley, New York (1958)

[2] R. S. Stein, J. J. Keane, F. H. Norris, F. A. Bettelheim and P. R. Wilson. *Ann N.Y. Acad. Sci.*, **83**, 37 (1959)

[3] R. S. Stein and J. J. Keane. *J. Polymer Sci.*, **17**, 21 (1955)

[4] J. J. Keane and R. S. Stein. *J. Polymer Sci.*, **20**, 327 (1958)

[5] R. S. Stein, S. N. Stidham and P. R. Wilson. *ONR Technical Rept. No. 34*, Project 356–378, Dept. of Chemistry, University of Massachusetts, Amherst (July 10th, 1961)

[6] P. Flory and A. D. McIntyre. *J. Polymer Sci.*, **18**, 592 (1955)

[7] M. Goldstein and E. R. Michalik. *J. Appl. Phys.*, **26**, 1450 (1955)

[8] R. S. Stein and P. R. Wilson. *J. Appl. Phys.*, in press

[9] A. Plaza and R. S. Stein. *J. Polymer Sci.*, **40**, 267 (1959)

[10] R. S. Stein and M. B. Rhodes. *J. Appl. Phys.*, **31**, 1873 (1960)

[11] P. R. Wilson and R. S. Stein. *ONR Technical Rept. No. 35*, Project 356–378, Dept. of Chemistry, University of Massachusetts, Amherst (July 25th, 1961)

[12] A. Gunier, G. Fournet, C. Walker and K. Yudowitch. *Small Angle Scattering of X-Rays*, p. 29, Wiley, New York (1955)

[13] A. Gunier, G. Fournet, C. Walker and K. Yudowitch. *Small Angle Scattering of X-Rays*, p. 56, Wiley, New York (1955)

[14] R. S. Stein, S. N. Stidham and P. R. Wilson. *ONR Technical Rept. No. 36*, Project 356–378, Dept. of Chemistry, University of Massachusetts, Amherst (August 10th, 1961)

[15] W. Hughes and C. A. Taylor. *J. Sci. Instr.*, **30**, 105 (1953); and references cited therein

[16] P. R. Wilson, S. Krimm and R. S. Stein. *J. Phys. Chem.*, **65**, 1749 (1961)

[17] A. Keller. *J. Polymer Sci.*, **17**, 291 (1955); **39**, 151 (1959)

[18] F. Price. *J. Polymer Sci.*, **37**, 71 (1959); **39**, 139 (1959)

[19] H. D. Keith and F. J. Padden. *J. Polymer Sci.*, **39**, 101, 123 (1959)

[20] R. J. Clark, R. L. Miller, R. S. Stein and P. R. Wilson. *J. Polymer Sci.*, **42**, 275 (1960)

[21] R. S. Stein and A. Plaza. *J. Polymer Sci.*, **45**, 519 (1960)

[22] S. W. Hawkins and R. B. Richards. *J. Polymer Sci.*, **4**, 515 (1949)

[23] M. B. Rhodes and R. S. Stein. *J. Polymer Sci.*, **45**, 521 (1961)

[24] P. Debye and A. Bueche. *J. Appl. Phys.*, **20**, 518 (1949)

[25] F. H. Norris and R. S. Stein. *J. Polymer Sci.*, **27**, 87 (1958)

[26] M. B. Rhodes and R. S. Stein. *ONR Technical Rept. No. 29*, Project 356–378, Dept. of Chemistry, University of Massachusetts, Amherst (February 13th, 1961); *J. Appl. Phys.*, **32**, 2344 (1961)

[27] C. R. Lindegren. *J. Polymer Sci.*, **50**, 181 (1961)